Liquid Crystals
Publication details, including instructions for authors and subscription information:
http://www.informaworld.com/smpp/title~content=t713926090

Solid state crystalline and liquid crystalline structure of semifluorinated 1-bromoalkane compounds

Jianguo Wang; Christopher K. Ober

Online publication date: 06 August 2010

To cite this Article Wang, Jianguo and Ober, Christopher K.(1999) 'Solid state crystalline and liquid crystalline structure of semifluorinated 1-bromoalkane compounds', Liquid Crystals, 26: 5, 637 — 648
To link to this Article: DOI: 10.1080/026782999204688
URL: http://dx.doi.org/10.1080/026782999204688

LIQUID CRYSTALS, 1999, VOL. 26, NO. 5, 637–648

Solid state crystalline and liquid crystalline structure of semifluorinated 1-bromoalkane compounds

JIANGUO WANG and CHRISTOPHER K. OBER*

Department of Materials Science and Engineering, Cornell University, Bard Hall, Ithaca, NY 14853-1501, USA

(*Received 5 November 1998; accepted 7 November 1998*)

A series of semifluorinated 1-bromoalkane (SFBA) mesogens have been synthesized and characterized to better understand their solid state crystalline and liquid crystalline structures. In the solid state, the local conformation of the fluorocarbon segments becomes disordered once the fluorocarbon chain reaches a length above eight CF_2 units. This is evident from the pronounced decrease of molar melting enthalpy. An increasing amount of helix and helix reverse conformations and increasingly disordered packing can also be observed with each addition of a fluorocarbon segment. X-ray diffraction peaks in the small angle region can be indexed by a tilted, two dimensional layered (herring bone) structure. The crystal structure is similar to a type of plastic crystal in which the amphiphilic character is clear, because the two segments of fluorocarbon and hydrocarbon are almost immiscible. Heating of $F(CF_2)_{12}(CH_2)_{10}Br$ leads to a transition from plastic crystal to smectic B, as revealed by time-resolved XRD and FTIR analysis. At this solid-to-liquid transition temperature, conformational analysis confirmed an onset of the CH_2 *gauche* conformation within the hexagonal lattice, most likely due to changes occurring in the hydrocarbon segment, and a sudden increase of helix defects along the fluorocarbon segment. The disordered helix rigid-rod structure of the fluorocarbon segment and its poor compatibility with the hydrocarbon segment play an important role in the crystalline solid and liquid crystalline structures.

1. Introduction

Organic fluorine chemistry has achieved significant success during recent years. Based on new fluoromonomers, many fluorinated polymer materials have been developed and are used extensively because of their superior thermal, chemical and antioxidation stability, as well as lower adhesion, dielectric constant, refractive index and flammability characteristics [1, 2]. Considering the molecular and supermolecular structures of commercial polyethylene and polytetrafluoroethylene (PTFE) polymers, it is clear that the excellent properties of PTFE arise mainly from the higher C–F single bond energy ($552\,kJ\,mol^{-1}$) with rigid-rod helix conformation, compared with the C–H bond ($338\,kJ\,mol^{-1}$) with its flexible zig-zag conformation [1].

Semifluorinated alkanes, $F(CF_2)_m(CH_2)_nH$ (referred to in this paper as F*m*H*n*) can be thought of as miniblock oligomers of a hydrocarbon and perfluorocarbon. These simple compounds provide an interesting topic for both theoretical research and materials application. Firstly, such miniblocks are constructed from two entirely incompatible segments, when $m > 8$. Therefore, the well-controlled structure of the low molar mass semifluorinated alkanes offers a suitable model in the study of the block copolymers. Secondly, the carbon segments become stiffened by the full fluorine substitution to give the fluorocarbon segment a rigid rod character. The connection of a flexible hydrocarbon spacer may lead to liquid crystalline behaviour in the molecule if the perfluorocarbon chain is greater than a critical length/width ratio. From materials design considerations, the poor solubility of fluorocarbons has strongly limited their processability. By introducing a flexible tail this problem is reduced and by using end-functionalized semifluorinated compounds one can synthesize a variety of side chain fluorinated materials to tailor the structure and properties of fluorine-containing materials.

The first paper dealing with the detailed synthesis and structure of semifluorinated alkanes was that of Rabolt and Twieg [3]. A longitudinal acoustical mode (LAM) study using Raman spectroscopy drew a preliminary picture of the structures as forming two connected stiff rods. Later, they recognized that the packing of semifluorinated *n*-alkanes is very complex as measured by small angle X-ray scattering [4]. The shorter hydrocarbon segments undergo antiparallel packing whereas longer hydrocarbon blocks prefer bilayered packing. In addition, a solid–solid transition [5] was observed which

*Author for correspondence.

Journal of Liquid Crystals ISSN 0267-8292 print/ISSN 1366-5855 online
http://www.tandf.co.uk/JNLS/lct.htm
http://www.taylorandfrancis.com/JNLS/lct.htm

was assigned to the translation of the molecules along their axes via a simple screw motion, whereupon they enter a rotator phase and melt in a manner similar to that observed with *n*-alkanes. Viney *et al.* and Mahler *et al.* [6–8] showed that the same transition was a crystalline or liquid crystalline to high order smectic (E, B or G)-like transition. Recently, solid state CP/MAS NMR experiments by Höpkin *et al.* [9] proved that the *gauche/trans* conformation ratio of hydrocarbon segments in semifluorinated alkanes above their transition temperature is similar to that for liquid paraffin. From morphology investigations, they suggested that molecules crystallized from solution have a very high order. Upon heating, an irreversible transition to a low ordered modification occurs which may be caused by formation of concentric lamellae from the normal layered lamellae in this miniblock material [10]. It is clear that, although the semifluorinated alkanes have a very simple structure, many basic questions remain because of uncertain interpretation of the experimental results.

In this study, a family of semifluorinated 1-bromoalkanes with different fluorocarbon ($m = 8$, 10, 12 CF_2) and hydrocarbon ($n = 2$, 4, 6, 10 CH_2) lengths were synthesized (see the scheme). Detailed characterization of the solid and liquid crystal structure of these compounds helps in understanding not only the structure of semifluorinated alkanes but also the structure of semifluorinated side chain polymers. Applications such as the creation of low surface energy materials by self-assembly of semifluorinated side chains in ionene and block copolymers have been discussed elsewhere [11].

2. Experimental

2.1. *Materials*

3-Butene-1-ol (99%), 4-butene-1-ol (99%), 5-hexene-1-ol (99%), 9-decene-1-ol (98%), 2.0M borane/dimethylsulphide in tetrahydrofuran, tributyltin hydride, carbon tetrabromide (99%), and triphenylphosphine (99%) were used as received from Aldrich. Azoisobutyronitrile (AIBN, Merck) was recrystallized from acetone/methanol (1:1) at 0°C. Perfluorooctyl iodide (97% min.), perfluorodecyl iodide, perfluorododecyl iodide and 1H, 1H, 2H, 2H-perfluorodecane (97% min.) purchased from PCR Inc. (Gainesville) were used without any further purification.

Semifluorinated 1-bromoalkanes were synthesized by a procedure described in the scheme. The ω-perfluoroalkyl-alcohols were prepared by a known anti-Markovnikov radical addition reaction [12] of 1-iodoperfluorocarbon with ω-alkene-1-ol. After dehalogenation, the alcohol was converted to the corresponding bromide by reaction with triphenylphosphine/carbon tetrabromide.

2.1.1. *General procedure for the synthesis of ω-perfluoroalkyl-alkanols: $F(CF_2)_m(CH_2)_nOH$ ($m = 8$, 10, 12; $n = 4$, 5, 6, 10)*

Semifluorinated alkanols were synthesized by a radical addition of perfluoroalkyl iodide with ω-alkene-1-ol followed by dehalogenation. In a 100 ml three-necked flask equipped with condenser, bubbler, nitrogen inlet and magnetic stirrer, was placed 30 mmol (16.38 g) of perfluorooctyl iodide and 45 mmol (3.25 g) 3-butene-1-ol and the mixture heated to 80°C. 75 mg AIBN was then added in small portions over 45 min and reacted for an additional 5 h with constant stirring. With perfluorodecyl iodide and perfluorododecyl iodide, the reaction was carried out at 90°C and 100°C respectively in order to keep the reaction mixture in the liquid state. The crude iodinated product was heated under reduced pressure to remove excess ω-alkene-1-ol and any low boiling point substances. Direct dehalogenation was then accomplished by adding 10 ml toluene, 3 mmol AIBN and 60 mmol of tri-*n*-butyltin hydride and heating at 80°C for 18 h. Then the solution was poured into 200 ml methanol to decompose the excess tributyltin hydride. The methanol was removed under vacuum and the product recrystallized from toluene at − 15°C. Finally, all

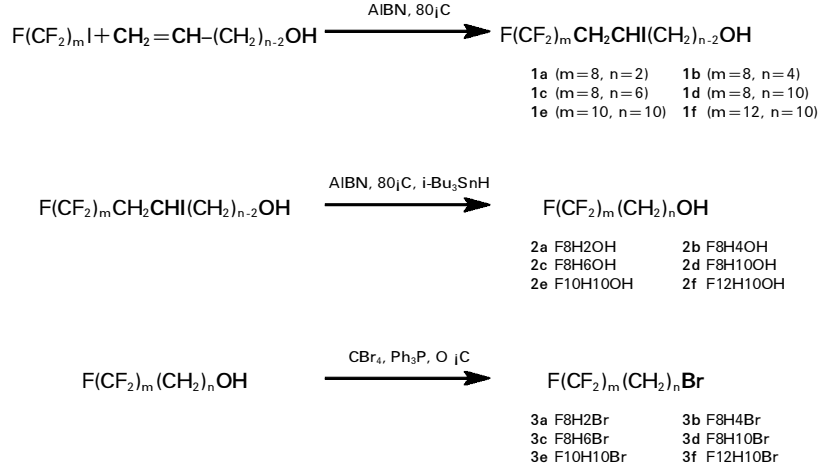

Scheme. Synthesis of semifluorinated 1-bromoalkanes.

products were sublimed under 0.2 mm Hg at a temperature just below their melting point. The yield varied from 68 to 75%, calculated from the perfluoroalkyl 1-iodide. The purity was checked by NMR and by comparison with previously reported melting points [4, 9].

Compound **2b**: ^{1}H NMR ($CDCl_3$ δ in ppm), 1.30 (t, 1H, $CH_2\underline{OH}$), 3.70 (q, 2H, $\underline{CH_2}OH$), 1.69 (4H, $\underline{CH_2}CH_2CH_2OH$), 2.12 (2H, $CF_2\underline{CH_2}$). ^{19}F NMR ($CDCl_3$, δ in ppm ref. as CF_3Cl), − 81.4 (CF3), − 126.6 ($CF_3\underline{CF_2}$), − 123.2 ($CF_3CF_2\underline{CF_2}$), − 122.3 ($CF_3CF_2CF_2\underline{(CF_2)_3}$), − 124.0 ($\underline{CF_2}CF_2CH_2$), − 114.9 ($\underline{CF_2}CH_2$).

Compound **2c**: ^{1}H NMR ($CDCl_3$, δ in ppm), 1.35 (t, 1H, CH_2OH), 1.40 (4H, $(\underline{CH_2})_2CH_2CH_2OH$), 1.60, 1.57 (4H, $CF_2CH_2\underline{CH_2}$, and $\underline{CH_2}CH_2OH$), 2.07 (2H, CF_2CH_2), 3.64 (2H, $\underline{CH_2}OH$).

Compound **2d**: ^{1}H NMR ($CDCl_3$, δ in ppm), 1.36 (1H, $CH_2\underline{OH}$), 1.39 (12H, $(\underline{CH_2})_6$ CH_2CH_2OH), 1.56 (4H, $CF_2CH_2\underline{CH_2}$, and $\underline{CH_2}CH_2OH$), 2.07 (2H, CF_2CH_2), 3.64 (2H, $\underline{CH_2}OH$).

Compound **2e**: same as **2d**.

Compound **2f**: same as **2d**.

2.1.2. *General procedure for synthesis of ω-perfluoroalkyl 1-bromoalkanes*

In a 100 ml round-bottomed flask, 0.01 mol (4.90 g) of compound **2a** and 0.015 mol (4.97 g) of carbon tetrabromide were dissolved in a mixture of 10 ml THF and 20 ml CH_2Cl_2 and cooled to − 5°C in an ice bath; 0.015 mol triphenylphosphine (3.93 g) was then added in small portions over 15 min. The reaction mixture was maintained at − 5°C for 1 h with an additional 6 h stirring at room temperature. During the reaction, a white precipitate of triphenyl phosphine oxide was gradually formed and the solvent became slightly pink due to formation of free bromine. The solution was evaporated and the product extracted four times with 10 ml portions of diethyl ether. The ether fraction containing product **3a** was collected and purified by reduced pressure distillation (yield 4.41 g, 79%) at 40–50°C, 0.5–1 mm Hg. Compounds **3b**, **3c** and **3d** were prepared in the same manner. Compounds **3e** and **3f** were prepared by reaction at 5–10°C to prevent the precipitation of ω-perfluoroalkyl alkan-1-ol. The brominated compounds were purified by passing through a short silica column to absorb the triphenylphosphine oxide. The final products were sublimed under a vacuum of 0.2 mm Hg.

Compound **3a**: ^{1}H NMR ($CDCl_3$ δ in ppm), 3.51 (t, 2H, CH_2Br), 2.70 (2H, CF_2CH_2), ^{19}F NMR ($CDCl_3$, δ in ppm ref. as CF_3Cl), ^{19}F NMR ($CDCl_3$, δ in ppm ref. to CF_3Cl), − 81.4 (CF_3), − 126.6 ($CF_3\underline{CF_2}$), − 123.2 ($CF_3CF_2\underline{CF_2}$), − 122.3 ($CF_3CF_2CF_2\underline{(CF)2_3}$), − 113.9 ($\underline{CF_2}CF_2CH_2$), − 114.7 ($\underline{CF_2}CH_2$), m.p. = 23–25°C.

Compound **3b**: ^{1}H NMR ($CDCl_3$, δ in ppm), 3.42 (t, 2H, CH_2Br), 2.09 (2H, CF_2CH_2), 1.95 (2H, $\underline{CH_2}CH_2Br$), 1.81 ($CF_2CH_2\underline{CH_2}$); m.p. = 32–34°C.

Compound **3c**: ^{1}H NMR ($CDCl_3$, δ in ppm), 3.41 (t, 2H, CH_2Br), 2.06 (2H, CF_2CH_2), 1.84 (2H, $\underline{CH_2}CH_2Br$), 1.60 (2H, $CF_2CH_2\underline{CH_2}$), 1.45 (4H, $CF_2CH_2CH_2\underline{CH_2CH_2}$); m.p. = 35–37°C.

Compound **3d**: ^{1}H NMR ($CDCl_3$, δ in ppm), 3.40 (t, 2H, CH_2Br), 2.06 (2H, CF_2CH_2), 1.84 (2H, CH_2CH_2Br), 1.60 (2H, $CF_2CH_2\underline{CH_2}$), 1.30 (12H, $CF_2CH_2CH_2\underline{(CH_2)}6$-$CH_2CH_2Br$); m.p. = 41–43°C.

Compound **3e**: ^{1}H NMR is same as **3d**; m.p. = 64–66°C.

Compound **3f**: ^{1}H NMR is same as **3d**; m.p. = 93–95°C.

2.2. *Characterization*

Differential scanning calorimetry (DSC) was performed on a Dupont 910 DSC with a Dupont 2000 controller. Samples of 6–8 mg were used with heating and cooling rates of 10°C min^{-1} and 5°C min^{-1}, respectively.

^{1}H and ^{19}F NMR spectra were measured on a Varian 200 instrument at 200 MHz, and at 188.2 MHz, respectively. All the spectra were measured at room temperature in deuteriated chloroform. Chemical shifts were referenced from TMS for ^{1}H NMR, CF_3Cl for ^{19}F NMR.

Polarizing optical micrographs were recorded on a Nikon microscope with a Mettler FP 80 hot stage and Nikon FX-35DX camera. Melting points, textures and transition temperatures were observed at a heating rate of 1°C min^{-1}.

Infrared spectra were obtained on a Mattson 2020 Galaxy series FTIR spectrometer with 4 cm^{-1} solution and 32 scans accumulation. Samples were pressed in a KBr tablet or cast on the NaCl crystal plate. Temperature dependent FTIR was studied by placing a FP 80 hot stage in the spectrometer. The samples were sandwiched between two pieces of NaCl plates and held at equilibrium at each temperature for 5 min.

Wide angle X-ray diffraction patterns were obtained using a SCINTAG θ-θ diffractometer equipped with a Ni-filtered Cu X-ray tube (K_α = 1.5418 Å) operated at 45 kV and 40 mA. Continuous scanning was used at a rate of 0.5°–1° min^{-1}. Single crystal Laué diffraction patterns were recorded with plate film with a typical exposure time of 12 h. Time-resolved X-ray experiments were performed at the Cornell High Energy Synchrotron Source (CHESS) at an X-ray wavelength of 0.908 Å; the diffraction patterns were collected with a CCD camera for 5 s with a 92 mm sample-to-detector distance and a 5°C min^{-1} heating rate.

3. Results and discussion

3.1. *Synthesis*

The synthesis of ω-perfluoroalkyl alcohols by free radical addition of a perfluoroalkyl iodide to ω-hydroxy

alkenes was carried out in good agreement with the procedure reported by Höpken *et al.* [12]. In order to eliminate possible side reactions during dehalogenation, excess ω-alkan-1-ol was distilled off before reduction with tributyltin hydride. The bromination reaction ran smoothly using excess (50–100%) carbon tetrabromide and triphenylphosphine at − 5 to 10°C. The conversion of hydroxide to bromide was complete after 6 to 8 h as monitored by ^{1}H and ^{19}F NMR. If the reaction temperature was increased to 40°C, conversion of the alcohol to the corresponding bromide was limited to about 80%. The products were readily purified by a short (*c.* 15 cm) silica column with diethyl ether as the elution solvent. High purity ω-perfluoroalkyl bromides were obtained by distillation or sublimation.

3.2. *Solid state structure of ω-perfluoroalkyl 1-bromoalkanes*

Although the structure of semifluorinated alkanes has been extensively discussed, a detailed analysis of these compounds is far from clear because single crystal structures are unavailable and even their wide angle X-ray diffraction peaks have not been indexed. This situation arises mainly from the complex structure of the fluorocarbon segment. For example, even the most familiar fluorocarbon material such as polytetrafluoroethylene (PTFE) has a very complex phase diagram [13–15]. Below 19°C, PTFE has a triclinic or pseudo-hexagonal phase ($a = 9.6$ Å, $b = 5.6$ Å, $c = 16.9$ Å) with a 13/6 helical conformation; an intermediate phase forms between 19 and 30°C, and above 30°C a hexagonal phase ($a = 5.66$ Å, $c = 19.5$ Å) is found in the form of a 15/7 helix. At high pressure above 4.5 kbar, PTFE changes to a hexagonal phase ($a = 5.61$ Å), $c = 6.75$ Å) with a planar zig-zag conformation like polyethylene. As discussed in a recent paper by Strobl *et al.* [16], the structure of perfluoroalkanes is even more complex than that of PTFE. The structure and molecular dynamics of perfluoro-*n*-eicosane exhibited three different solid state modifications, in which a monoclinic phase ($a = 9.65$ Å, $b = 5.7$ Å, $c = 28.3$ Å, $\beta = 97°$, 15/7 helix) is stable below 146 K. In the range 146–200 K an intermediate phase forms which above 200 K transforms into a rhombohedral phase ($a = 5.7$ Å, $c = 85$ Å, $\alpha = \beta = 90°$, $\gamma = 120°$).

To study the solid state structure of the semifluorinated bromides described in this paper, needle-like crystals of compounds **2a**, **2b**, and **2c** were grown from either the melt or from solution. All the crystals are very elastic at room temperature and can be bent or broken into small needles. From four cycle single crystal analysis, it is impossible to determine their structure owing to a lack of ideal diffraction data. Single crystal Laué diffraction patterns exhibit clear wide angle diffraction rings at 4.9–5.0 Å, including some sharp diffraction spots. These are characteristics typical of plastic crystals.

DSC results for **3a–f** are listed in table 1. Increasing the length of the hydrocarbon segment leads to a slight increase of melting point from 24.6°C (**3a**) to 44.0°C (**3d**). Apparently, the melting point is dominated by the length of the fluorocarbon groups, so that T_m increases from 44.0°C (F8H10Br)† to 70.7°C (F10H10Br) to 96.5°C (F12H10Br). The melting enthalpy shows a nearly linear increase with addition of each spacer methylene group going from 2 to 10. The melting enthalpy increase is about 3.1 kJ mol^{-1} per CH_2 which is close to that for the melting of hexagonally packed paraffin [17] but smaller than that for orthorhombic packing, *c.* 4–4.1 kJ mol^{-1} for polyethylene [18]. Surprisingly, melting enthalpy decreases from 38.5 to 21.9 kJ mol^{-1} when the number of CF_2 groups was increased from 8 to 12. Normally, if such analogues possess a similar crystal structure, the molar melting enthalpy increases with increasing molecular weight. This unusual phenomenon may indicate that the structure of the CF_2 groups become disordered which in turn influences the orderly packing of the CH_2 segment. Recent perfluorocarbon single crystal structure results imply that both the tendency to form a given crystal structure and the stability of a helical conformation are strongly dependent on molecular length. For example, perfluoroeicosane, $F(CF_2)_{20}F$, forms only a stable 15/7 helix conformation, even at very low temperatures, while PTFE forms a more twisted 13/6 helix. In contrast, above room temperature perfluoroeicosane forms a rotator phase with a helical conformation of ≈ 15/7 whereas PTFE forms its stable 15/7 helix. Early FTIR results indicated that small perfluorocarbons such as perfluorobutane and perfluorohexane existed in a stable zig-zag conformation [19] at low temperature. Even in PTFE, a planar conformation may

Table 1. Thermal properties of semifluorinated 1-bromoalkanes.

Compound	Structure	T_m/°C	ΔH_m/kJ mol^{-1}
3a	$F(CF_2)_8(CH_2)_2Br$	24.6	13.9
3b	$F(CF_2)_8(CH_2)_4Br$	34.8	20.8
3c	$F(CF_2)_8(CH_2)_6Br$	38.5	27.6
3d	$F(CF_2)_8(CH_2)_{10}Br$	44.0	38.5
3e	$F(CF_2)_{10}(CH_2)_{10}Br$	70.7	32.3
3f	$F(CF_2)_{12}(CH_2)_{10}Br$	80.1[a]	8.9
		96.5	21.9

[a] Plastic crystal to smectic B transition

†It is informative to refer to compounds **3** by the compositional codes listed in the scheme (e.g. F8H2Br for **3a**). Both types of identifier are used as appropriate in this paper.

coexist with the 15/7 helix conformation as reported by Masetti *et al.* [20].

Molecular vibration spectra, which detect the normal wagging and rocking modes of methylene groups [21] are very sensitive to local conformation. In order to examine ideas concerning conformation differences and defect formation with increasing number of CF_2 groups, FTIR spectra of semifluorinated 1-bromoalkanes were obtained and are plotted in figure 1. In the fingerprint region, a complex oscillation model has been developed for the 700–1100 cm^{-1} region of perfluoroalkanes as discussed recently by Snyder *et al.* [22]. In comparison, assignment of the 500–700 cm^{-1} region is relatively simple in that the isolated CF_2 wagging and rocking mode is sensitive to the local conformation of CF_2 groups and has been well assigned by extensive investigation of PTET [23, 24]. The peak of 648 cm^{-1} has been assigned to the CF_2 wagging vibration in the helical conformation of PTFE. This peak was also very strong in the F12H10Br and F10H10Br compounds, but present as a weak shoulder in F8H4Br, F8H6Br and F8H10Br.

According to assignment by Brown [25], a helix reversal (a right hand helix turning to a left hand helix), gives rise to a characteristic peak at 667 cm^{-1}. This peak can be found as a clear shoulder in F12H10Br and F10H10Br and as a very weak shoulder in F8H(4,6,10)Br. The strong peak at 667 cm^{-1} decreases significantly with increasing CF_2 length from 8 to 12. Based on the values of melting enthalpy, the CF_2 unit in F8H(4,6,10)Br must possess a highly ordered conformation, and we deduce that the peak at 667 cm^{-1} may be assigned to the wagging vibration of a CF_2 in-plane zig-zag conformation.

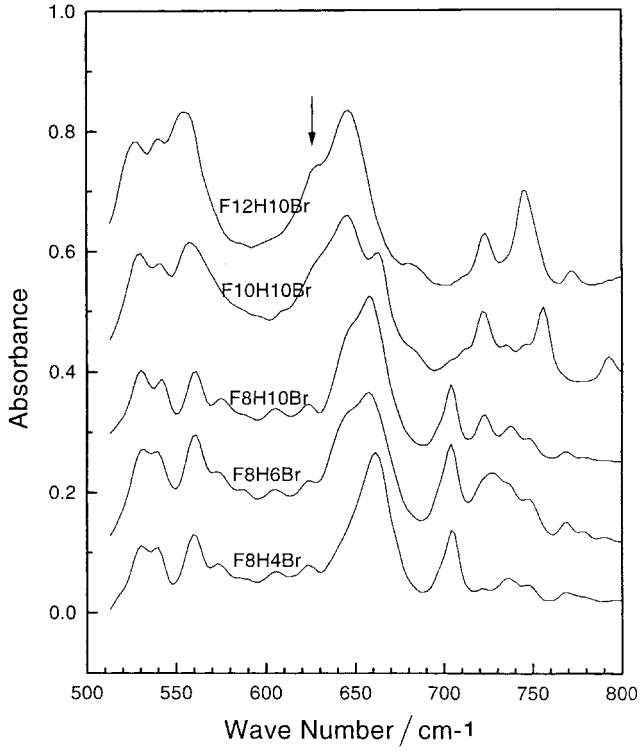

Figure 1. FTIR spectra of semifluorinated compounds.

The above analysis was also supported by FTIR investigations of PTFE by Brown, in which the planar conformation was detected by X-ray diffraction at high pressure (> 4.5 kbar). As evident in the original spectra [25] a remarkable decrease in peak intensity occurred at 648 cm^{-1} under 60 kbar, while the peak at 667 cm^{-1} became more intense; X-ray diffraction confirmed the formation of a zig-zag conformation. A quantitative determination of the conformation ratio between helix and zig-zag conformation. A quantitative determination of the conformation ratio between helix and zig-zag by FTIR in semifluorinated 1-bromoalkanes is difficult because the overlapping of Br–C stretching near 650 cm^{-1} interferes with any measurement. If we assign the peaks at 667 cm^{-1} as evidence of a zig-zag conformation, then the dominant conformation of the $F(CF_2)_8$ segment is the planar zig-zag conformation, while $F(CF_2)_{10}$ is a mixture of planar and helical conformations. The $F(CF_2)_{12}$ segment is dominated by helix conformations with some helix defects.

These conformational differences are clearly seen in the semifluorinated alcohols **2d** and **2e** because the overlapping Br–C stretch is absent. Therefore, the above features seem independent of the functional groups attached to the semifluorinated alkanes. It is well known that the driving force for helix formation in PTFE is the F-atom diameter which is larger than the *trans* length C–C–C (2.62 Å). A slight distortion of the C–C–C bond angle of about 12° (15/7 helix) can meet the requirement of lowering the interaction energy of neighbouring fluorine atoms. However, a planar conformation may be tolerated for short perfluoroalkanes, because the energy gained from increasing the bond C–C–C angle in the zig-zag conformation is compensated by minimizing the conformational energy. Another possible reason is that the stable zig-zag conformation in a hydrocarbon segment promotes formation of a zig-zag conformation in the perfluorocarbon segment. Consequently, the planar zig-zag and helix conformations coexist in the semifluorinated alkane making the structure complicated to analyse.

A miscibility study of equal molar blends of F8H10Br and F10H10Br by DSC and polarizing microscopy showed two distinct melting points and crystallization processes upon heating and cooling, which means that their bromide components **3d** and **3e** form immiscible crystals. These experiments provide further evidence of the conformational change with increasing CF_2 group length. This may indicate that the helical and planar conformations are thermodynamically immiscible because

the packing of the helix has a high stereo-selectivity similar to right/left helix packing.

The small angle X-ray diffraction study of these linear molecules provides useful information about molecular packing, since normally linear molecules tend to arrange in layered structures based on close packing theory. The diffraction patterns of semifluorinated compounds are shown in figure 2. In contrast to SAXS results of many linear molecules, more complex packing arrangements were found in these miniblocks. Typically, the first of several strong peaks cannot be easily indexed as either 0 0 1, 0 0 2 or 0 0 3 from regular layer diffraction of a one dimensional space group. On the other hand, only very weak second and third diffraction peaks can be observed for the semifluorinated 1-bromoalkanes. For compounds **3a** and **3b**, two identical first order diffraction peaks appeared with a 3–4 Å layer spacing. In order to compare d-spacings, the approximate molecular length of semifluorinated 1-bromoalkanes were calculated (table 2) according to the bond length and van der Waals radius in F–F and Br–Br atoms pairs.

Similar small angle diffraction data were found for SFA compounds; this was explained as either a mixture of head-to-head and head-to-tail packing [6] or an imperfect layer diffraction of the liquid crystalline state [8]. However, the diffraction data in table 2 cannot be interpreted by all the proposed structural models. A complete packing model for semifluorinated compounds must explain three observations. First, there are large cross-sectional area differences between CF_2 and CH_2 groups; this makes normal regular close packing of simple rods almost impossible. Secondly, the complex local conformations of CF_2 segments and CH_2 segments coexist in the solid state which makes it difficult to get detailed information by single crystal analysis. Thirdly, long CF_2 and CH_2 segments are almost immiscible, thus these miniblock oligomers have the characteristics of amphiphilic molecules or block copolymers in which the morphology strongly depends on composition, chain flexibility and thermal history.

With the aid of a powder X-ray diffraction program, it was possible to index all the small angle diffraction peaks in figure 2 by a planar lattice. The calculated assignment of the X-ray diffraction peaks was in good agreement with the X-ray experiments. A large lattice (30–50 Å) and absence of any symmetric features indicate a layered structure of low symmetry. The most plausible space groups to fit the observed diffraction peaks are the two dimensional space groups P_1 or P_2. Since the unit cell parameter is larger than the molecular length and smaller than the bilayer length, a non-centrosymmetric lamellar structure model is proposed in figure 3, in which the molecular plane is constructed of two alternating tilted layers, i.e. a typical ABABAB layered structure, in which the AB layers form antiparallel head-to-head packing. The different tilt angle gives rise to the first two orders of reflection. The 1 0 0 and 0 1 0 peaks are strongly depressed because of their head-to-head packing. That the 2 1 0 planar diffraction is the strongest peak may be because the molecular axis is oriented in this direction. The proposed structural model may correlate with the observation of a zig-zag morphology in rod-coil polymers such as poly(styrene-b-hexylisocyanate) block copolymers [26] because of their structural similarity.

WAXD curves of compounds **3d**, **3e** and **3f** are shown in figure 4. The diffuse halo at 5 Å reveals that these materials are not perfect crystals. From X-ray intensity analysis based on atomic diffraction factors, we know that the strongest diffraction peaks in the wide angle

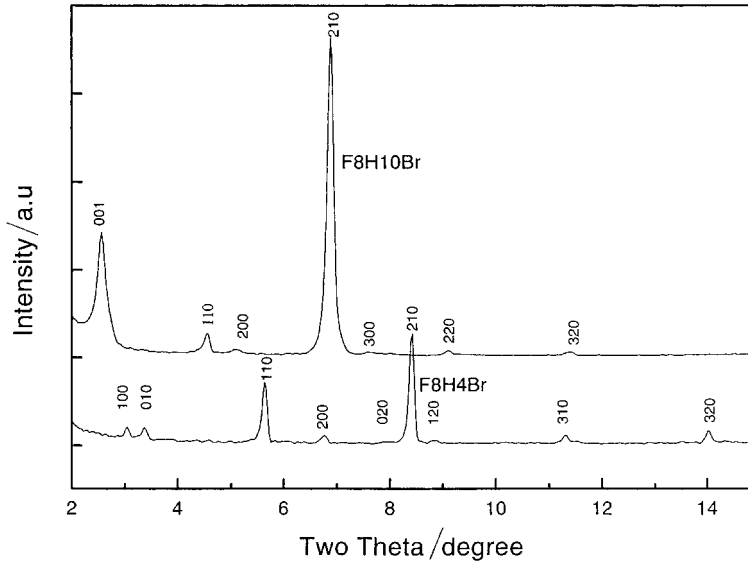

Figure 2. X-ray diffraction plot with indexing at small angle region.

Table 2. X-ray diffraction data and their index for semifluorinated 1-bromoalkanes: d-spacings in Å.

$F(CF_2)_8(CH_2)_4Br$			$F(CF_2)_8(CH_2)_6Br$			$F(CF_2)_8(CH_2)_{10}Br$			$F(CF_2)_{10}(CH_2)_{10}Br$			$F(CF_2)_{12}(CH_2)_{10}Br$		
Molecular length 18.5 Å Unit cell parameters $a = 34.4$ Å, $b = 30.3$ Å, $\gamma = 122.3°$			Molecular length 21.1 Å Unit cell parameters $a = 29.8$ Å, $b = 26.0$ Å, $\gamma = 111.3°$			Molecular length 26.1 Å Unit cell parameters $a = b = 41.8$ Å, $\gamma = 124.3°$			Molecular length 28.4 Å Unit cell parameters $a = b = 47.6$ Å, $\gamma = 125.6°$			Molecular length 30.6 Å Unit cell parameters $a = b = 52.2$ Å, $\gamma = 125.0°$		
d (obs.)	d (calc.)	$h\ k\ l$	d (obs.)	d (calc.)	$h\ k\ l$	d (obs.)	d (calc.)	$h\ k\ l$	d (obs.)	d (calc.)	$h\ k\ l$	d (obs.)	d (calc.)	$h\ k\ l$
29.1 (m)	29.1	100	27.8 (m)	27.8	100	34.5 (s)	34.5	100	39.1 (vs)	38.8	100	43.1 (vs)	42.8	100
26.1 (m)	26.1	010	24.3 (s)	24.2	010	19.5 (m)	19.5	110	21.6 (w)	21.8	110	24.0 (m)	24.1	110
15.70 (s)	15.70	110	15.61 (s)	15.65	110	17.28 (w)	17.27	200	19.53 (w)	19.35	200	15.92 (s)	15.82	210
14.55 (w)	14.54	200	13.04 (w)	12.96	1-20	12.85 (vs)	12.82	210	14.37 (vs)	14.30	210	12.03 (w)	12.05	220
13.05 (m)	13.06	020	12.14 (w)	12.11	020	11.56 (w)	11.51	300	13.04 (w)	12.90	300	9.58 (w)	9.59	230
10.53 (vs)	10.53	210	10.51 (vs)	10.51	210	9.72 (w)	9.76	220	10.78 (w)	10.88	220	8.02 (w)	8.03	330
10.05 (w)	10.07	120	9.86 (s)	9.87	120	7.77 (w)	7.77	320	8.67 (w)	8.66	320	6.87 (vw)	6.87	340
8.74 (w)	8.71	030	9.33 (w)	9.26	300				7.19 (w)	7.15	420			
7.82 (m)	7.82	310	8.12 (m)	8.07	030				6.18 (w)	6.20	430			
6.32 (m)	6.33	320	7.81 (m)	7.83	220									

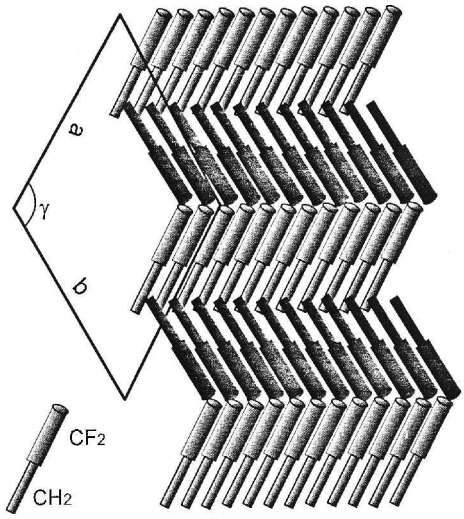

Figure 3. Scheme representing structural model of semifluorinated compounds.

region should derive from the CF_2 layer spacing. We can therefore estimate the crystal thickness by analysis of diffraction line width. Obviously, longer CF_2 segments present in the block unit will lead to less ordered CF_2 packing in the crystal. This result can be explained by the FTIR conformational analysis, because the longer CF_2 segments tend to form more disordered helical conformations. The disordered packing from wide angle X-ray diffraction is also consistent with a complex packing model derived from small angle X-ray analysis. Therefore, combining the SAXS, WAXD and FTIR results, and taking into account the elastic behaviour of these compounds, the semifluorinated 1-bromoalkanes behave like a plastic crystal at room temperature.

3.3. *Liquid crystal behaviour of F12H10Br*

Compound F12H10Br showed a strong transition before isotropic melting at 80.1°C (figure 5). The corresponding texture from polarizing light microscopy at 85°C is shown in figure 6. The biaxial character of the liquid crystal and its highly birefringent behaviour

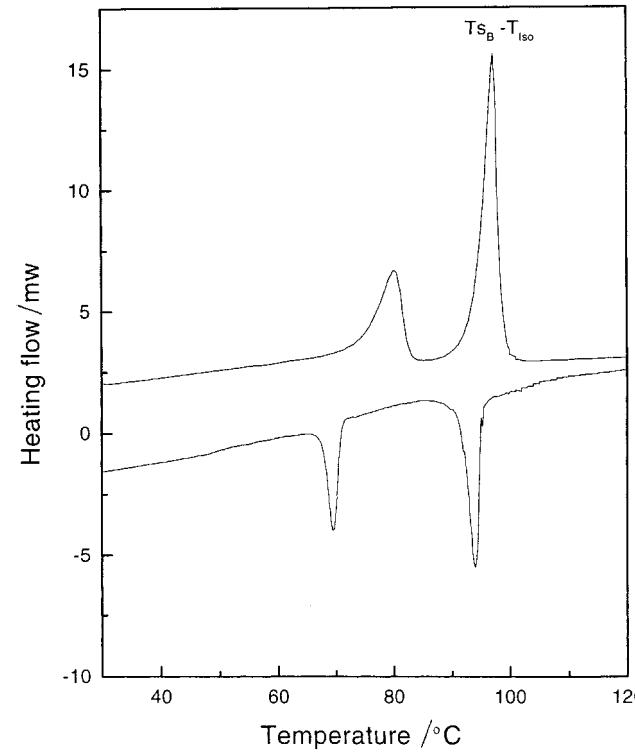

Figure 5. Heating and cooling DSC traces of the liquid crystal transition of $F(CF_2)_{12}(CH_2)_{10}Br$.

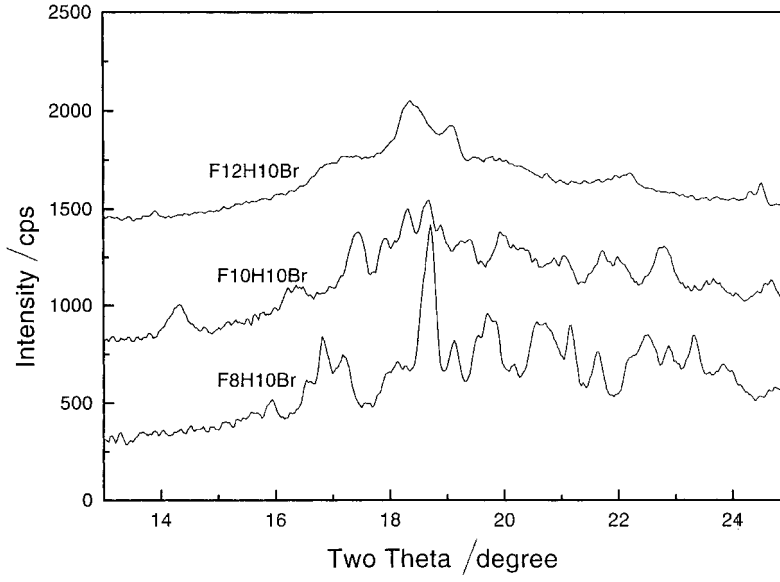

Figure 4. X-ray diffraction plots of semifluorinated 1-bromoalkanes at wide angle region.

Figure 6. Polarizing optical micrograph of $F(CF_2)_{12}(CH_2)_{10}Br$ at 85°C.

correspond to the mixture of focal-conic and mosaic textures observed in highly ordered smectic phases.

The transition enthalpy of 8.9 kJ mol is larger than that of many crystal-to-smectic transitions. Although similar transitions have been extensively discussed in many publications [5–10], the transition mechanism is still unclear. From these reports, two factors apparently play important roles in the transition. First a minimum CF_2 length, generally above 8 CF_2 units, is necessary. This length is just enough to start the formation of the helix conformation and the helix reversal defect. From the viewpoint of liquid crystal theory, that length of CF_2 unit may be just above the axial ratio for a rigid-rod mesogen. Secondly, from the transition entropy, the transition must include a huge conformational change which is larger than for normal LC–LC transitions [6, 27].

Conformational changes during the transition were followed by measuring the FTIR spectrum of F12H10Br while raising its temperature (figure 7). Using the conformational study of polyethylene by Snyder [21] we could follow the conformational changes during the transition. By plotting the relationship between absorbance and temperature of these peaks, we found that at the transition temperature the peaks at 1470 and 720 cm^{-1} due to the *tt* conformation of $(CH_2)_{m>2}$, and the helix conformation absorption of CF_2 at 648 cm^{-1}, decrease sharply. In contrast, the *gg* conformation of $(CH_2)_{m>2}$ at 1390 and 860 cm^{-1}, and the helix reversal defect peaks at 626 cm^{-1}, increase at the transition temperature. This becomes clear when comparing the FTIR spectra at 70, 80 and 90°C in figure 7. The conformational change in the hydrocarbon segment occurs in the temperature range 80–90°C (rather than at 90–100°C expected from the CH_2 melting process) and occurs below the clearing temperature. In contrast, the most significant conformational change of the fluorocarbon segment occurs just at the temperature of clearing transition.

In order to understand the nature of this transition, time-resolved WAXD data were recorded at the Cornell High Energy Synchrotron Source (CHESS). The two dimensional diffraction patterns were digitally converted to one dimensional patterns; the results are shown in figure 7. Below the transition, compound **3f** is crystalline, exhibiting several strong diffraction peaks including 4.96 and 5.11 Å, with a broad diffracted halo illustrated by a localized three dimensionally ordered structure. The strongest peak is generally assigned to hexagonal packing of CF_2 groups. The layer distance is 43.8 Å. Above 90°C, only one broad peak appears at 5.06 Å which becomes sharper when compared with the room temperature pattern. Therefore, above the transition the longitudinal separation of the CF_2 groups is still ordered, and even more uniform than at lower temperature. In principle, molecular movement is faster at high temperature, therefore this strong diffraction peak for the CF_2 spacing is possible only if molecular rotation is predominately about the $-(CF_2)_m-$ longitudinal axis. At room temperature some of the localized conformation and defect structures will give rise to broad diffraction peaks. At small angle, a new reflection emerges at 31.8 Å which is exactly equal to the length of the molecule. The 13.7 Å difference in *d*-spacing can be explained as the melting transformation of CH_2 from head-to-head packing in a head-to-head bilayer to an interdigitated packing of the fluorocarbon segment. By considering a combination of X-ray analysis and FTIR results, the transition can be regarded as a plastic crystalline to smectic B transition.

In the solid state, the molecular structure and especially the local conformation of the fluorocarbon segment is governed by the length of the CF_2 unit. When the CF_2 unit contains more than eight carbon atoms, a planar conformation will gradually change to a 15/7 helix conformation in which helical defects exist in the fluorocarbon segment. This fact suggests a rigid-rod

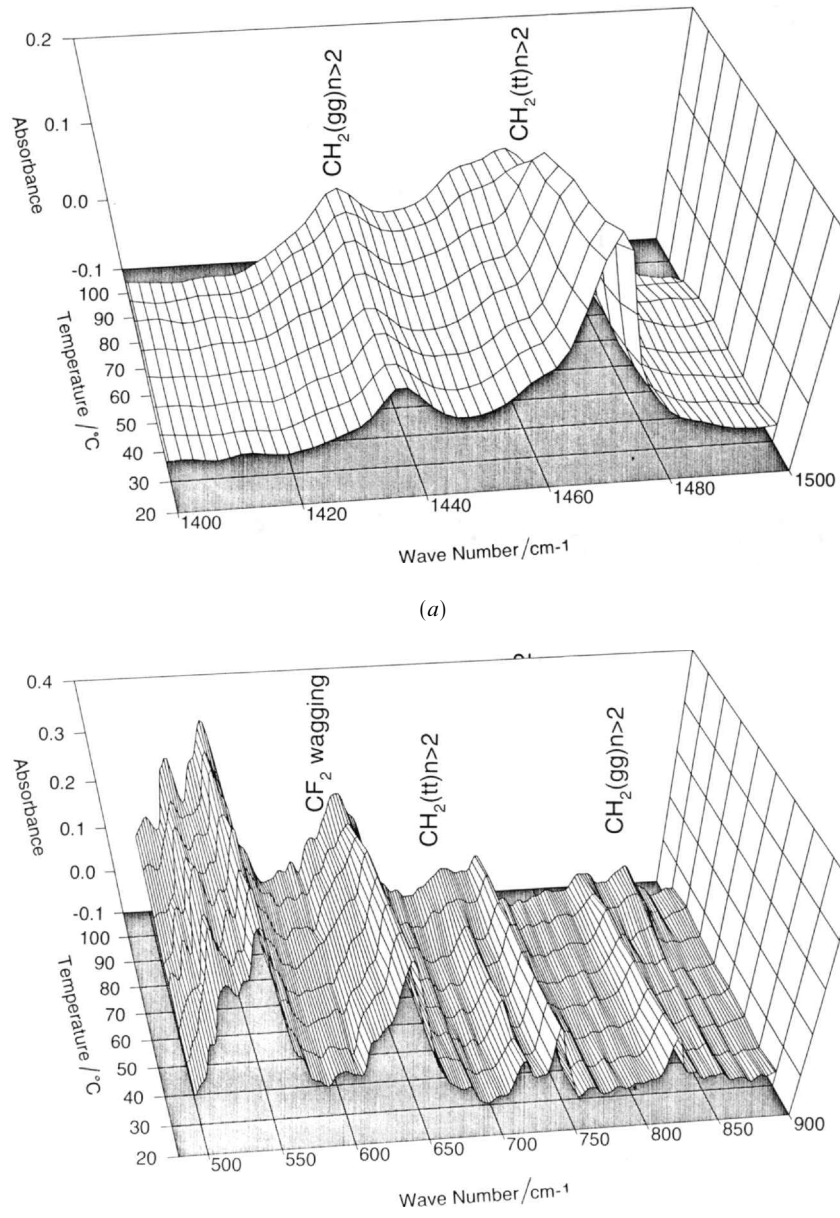

Figure 7. Time-resolved FTIR spectra of $F(CF_2)_{12}(CH_2)_{10}Br$.

character to the CF_2 segment because very small entropy changes occur during the melting process. Unlike normal linear alkanes, molecular packing of this miniblock produces a disordered lamellar structure owing to the strong aggregation of the CF_2 units. On the other hand, the self-organization of these rod block molecules make it possible to form highly ordered smectic B liquid crystal phases.

4. Conclusion

In summary, these simple semifluorinated 1-bromoalkanes have very complicated structures which can best be described from the dual viewpoint of liquid crystal and block copolymers. The local conformation of the fluorocarbon segments strongly depends on the length of the unit. From DSC, FTIR and X-ray analysis, it is observed that, below eight CF_2 units, the fluorocarbon segments mainly form a zig-zag conformation. Above eight CF_2 units, slight distortion at each CF_2 leads to a helix conformation. In addition, the helix reverse (helix defect) concentration strongly increases with increasing number of CF_2 units. This structural modification gives the longer CF_2 segments rigid-rod characteristics, because of the small entropy change required for the solid to isotropic phase transition. Consequently, at room temperature, SFAB compounds are plastic crystals.

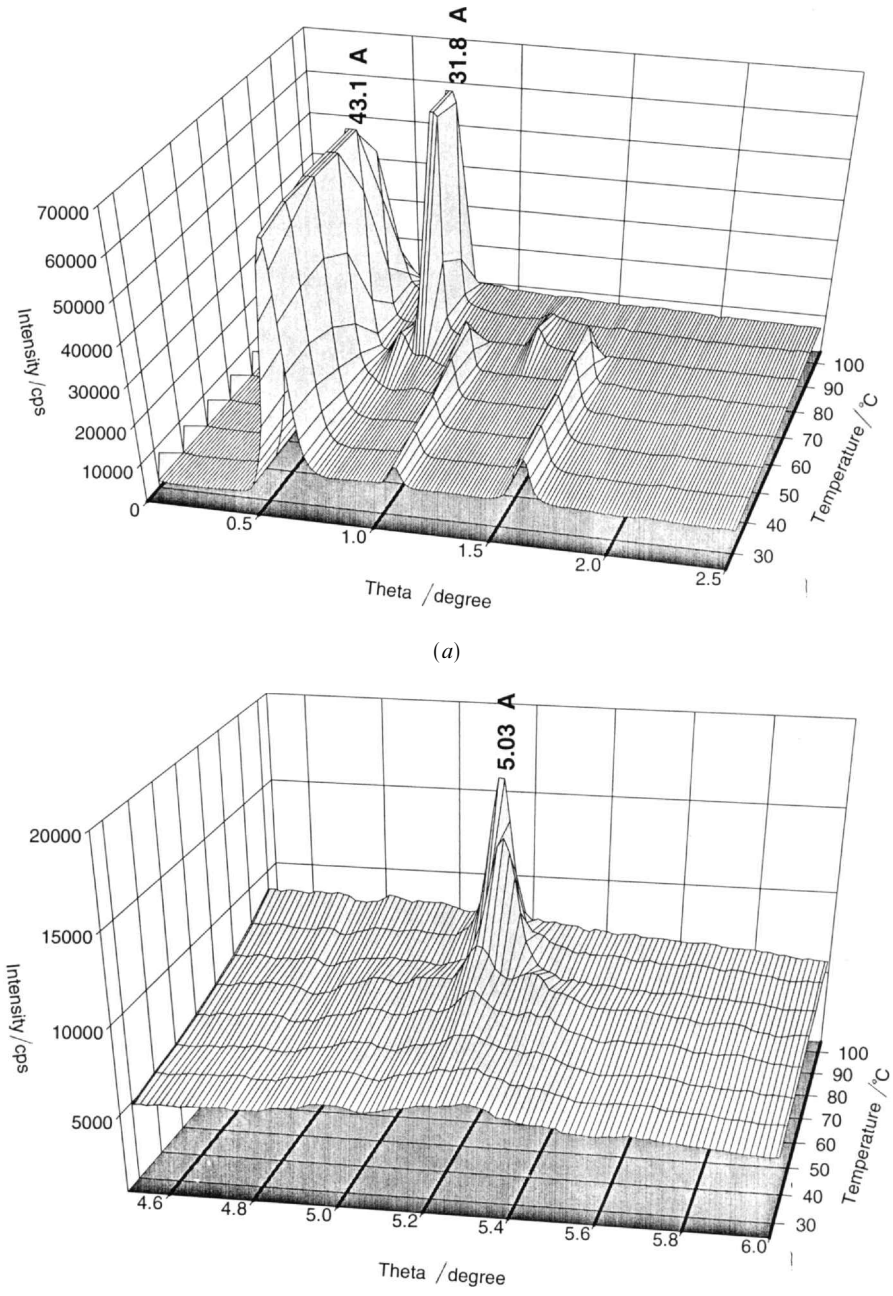

Figure 8. Time-resolved X-ray diffraction plots for $F(CF_2)_{12}(CH_2)_{10}Br$.

X-ray analysis shows that, apart from the many layered structures, these crystals are packed in a largely planar lattice, in which the structure can be regarded as two tilted layers arranged in a herringbone fashion, the layers being constructed of close-packed hydrocarbon and fluorocarbon segments. Upon heating, $F(CF_2)_{12}(CH_2)_{10}Br$ undergoes a plastic crystal to smectic B transition as shown from time-resolved X-ray and FTIR analysis. Above the transition temperature, the hydrocarbon chains are melted and the fluorocarbon units are packed into hexagonal cylinders where the local conformation becomes disordered.

This research was supported by the Office of Naval Research, Grant No. N00014-92-J-1246. Many valuable discussions with Prof. E. J. Kramer are gratefully acknowledged. We thank Dr H. Körner and Prof. M. A. Levelut for their enlightened discussion of the

X-ray diffraction results. We also thank the National Science Foundation for partial support of this work through grant DMR-9321573.

References

[1] Gangal, S. V., 1989, *Encyclopedia of Polymer Science and Engineering*, 2nd Edn, edited by H. E. Mark, N. M. Bikales, C. G. Overberger, and G. Menges (New York: Wiley), Vol. 16, pp. 626–642.
[2] Calson, D. P., and Schmiegel, W., *Ullmann's Encyclopedia of Industrial Chemistry* (Weinheim: VCH), Vol. A11, pp. 393–429.
[3] Twieg, R., and Rabolt, J. F., 1983, *J. Polym. Sci. Polym. Lett. Ed.*, **21,** 901.
[4] Rabolt, J. F., Russell, T. R., and Twieg, R. J., 1984, *Macromolecules*, **17,** 2786.
[5] Russell, T. P., Rabolt, J. F., Twieg, R. J., and Siemens, R. L., 1986, *Macromolecules*, **19,** 1135.
[6] Mahler, W., Guillon, D., and Skoulios, A., 1985, *Mol. Cryst. liq. Cryst. Lett.*, **2,** 111.
[7] Viney, C., Russell, T. P., Depero, L. E., and Twieg, R. J., 1989, *Mol. Cryst. liq. Cryst.*, **168,** 63.
[8] Viney, C., Twieg, R. J., Russell, T. P., and Depero, L. E., 1989, *Liq. Cryst.*, **5,** 1783.
[9] Höpken, J., Pugh, C., Richtering, W., and Möller, M., 1988, *Makromol. Chem.*, **189,** 911.
[10] Höpken, J., and Möller, M., 1992, *Macromolecules*, **25,** 2482.
[11] Wang, J.-G., and Ober, C. K., 1997, *Macromolecules*, **30,** 7560; Wang, J.-G., Mao, G. P., Ober, C. K., and Kramer, E. J., 1997, *Macromolecules*, **30,** 1906.
[12] Höpken, J., Möller, M., and Boileau, S., 1991, *New polym. Mater.*, **2,** 239.
[13] Bunn, C. W., and Howells, E. R., 1954, *Nature*, **174,** 549.
[14] Flack, H. D., 1972, *J. Polym. Sci., A-2*, **10,** 1799.
[15] Starkweather, Jr, H. W., Zoller, P., Jones, G. A., and Vega, A. J., 1982, *J. Polym. Sci., Polym. Phys. Ed.*, **20,** 751.
[16] Schwickert, H., Strobl, G., and Kimmig, M., 1991, *J. chem. Phys.*, **95,** 2800.
[17] Broadhurst, M. G., 1962, *J. Res. natl. Bur. Stand. A*, **66,** 241.
[18] Brandrup, J., and Immergut, E. H., in *Polymer Handbook*, 3rd Edn, John Wiley & Sons, New York, 1989.
[19] Compos-Vallette, M., and Rey-Lafon, M., 1983, *J. mol. Struct.*, **101,** 23; Marx, A., Krüger, J. K., Kirfel, A., and Unruh, H.-G., 1990, *Phys. Rev. B*, **42,** 6642.
[20] Masetti, G., Cabassi, F., Morelli, G., and Zerbi, G., 1973, *Macromolecules*, **6,** 700.
[21] Snyder, G. R., 1967, *J. chem. Phys.*, **47,** 1316.
[22] Hsu, S. L., Reynolds, N., Bohan, S. P., Strauss, H. L., and Snyder, R. G., 1990, *Macromolecules*, **23,** 4565.
[23] Liang, C. Y., and Krimm, S., 1956, *J. chem. Phys.*, **25,** 563.
[24] Moynihan, R. E., 1959, *J. Am. chem. Soc.*, **81,** 1045.
[25] Brown, R. G., 1964, *J. chem. Phys.*, **40,** 289.
[26] Marx, A., Krüger, J. K., Kirfel, A., and Unruh, H.-G., 1990, *Phys. rev. B*, **42,** 6642.
[27] Jariwala, C. P., and Mathias, L. J., 1993, *Macromolecules*, **26,** 5129.